ELSEVIER

Journal of Biomechanics 38 (2005) 2102–2112

JOURNAL OF BIOMECHANICS

www.elsevier.com/locate/jbiomech
www.JBiomech.com

Design and demonstration of a dynamometric horseshoe for measuring ground reaction loads of horses during racing conditions

Elizabeth S. Roland[a], Maury L. Hull[a,b,*], Susan M. Stover[c]

[a]*Biomedical Engineering Program, College of Engineering, University of California, One Shields Avenue, Davis, CA 95616, USA*
[b]*Department of Mechanical Engineering, College of Engineering, University of California, One Shields Avenue, Davis, CA 95616, USA*
[c]*Department of Anatomy, Physiology, and Cell Biology, School of Veterinary Medicine, University of California, One Shields Avenue, Davis, CA 95616, USA*

Accepted 24 August 2004

Abstract

Because musculoskeletal injuries to racehorses are common, instrumentation for the study of factors (e.g. track surface), which affect the ground reaction loads in horses during racing conditions, would be useful. The objectives of the work reported by this paper were to (1) design and construct a novel dynamometric horseshoe that is capable of measuring the complete ground reaction loading during racing conditions, (2) characterize static and dynamic measurement errors, and (3) demonstrate the usefulness of the instrument by collecting example data during the walk, trot, canter, and gallop for a single subject. Using electrical resistance strain gages, a dynamometric horseshoe was designed and constructed to measure the complete ground reaction force and moment vectors and the center of pressure. To mimic the load transfer surface of the hoof, the shape of the surface contacting the ground was similar to that of the solar surface of the hoof. Following static calibration, the measurement accuracy was determined. The root mean squared errors (RMSE) were 3% of full scale for the force component normal to the hoof and 9% for force components in the plane of the hoof. The dynamic calibration determined that the natural frequency with the full weight of a typical horse was 1744 Hz. Example data were collected during walking on a ground surface and during trotting, cantering, and galloping on a treadmill. The instrument successfully measured the complete ground reaction load during all four gaits. Consequently the dynamometric horseshoe is useful for studying factors, which affect ground reaction loads during racing conditions.

1. Introduction

Musculoskeletal injuries are the reason for over 80% of deaths in California racehorses (Johnson et al., 1994) and the leading cause of inability to train and race racehorses (Rossdale et al., 1985; Lindner and Dingerkus, 1993; Hill et al., 2001). Although injuries appear to occur suddenly, the history of activity and equipment used in the months preceding injury are known to affect the likelihood for injury. Factors such as training intensity (Estberg et al., 1998; Hill et al., 2001,2003) and horseshoe and hoof characteristics (Kane et al., 1996,1998; Balch et al., 2001; Hill et al., 2001) are believed to be important because they affect the frequency, intensity, and direction of loading.

To understand how the above factors contribute to the damage of musculoskeletal tissue, a means for measuring the ground reaction loads would be useful. One possible approach is a force plate embedded in the ground (Pratt and O'Connor, 1976; Steiss et al., 1982; Barrey, 1990; Hjerten and Drevemo, 1994; Barr et al., 1995; Roepstorff, 1997). Force plates are practical particularly for the walk and trot but are less practical for either the canter or gallop. With a stride length that exceeds the plate length by more than 6 m, it is difficult for horses traveling at a gallop to step in the center of the plate. Also the location of the center of pressure (COP) on the hoof cannot be determined directly.

*Corresponding author. Tel.: +1 530 752 6220; fax: +1 530 752 4158.
E-mail address: mlhull@ucdavis.edu (M.L. Hull).

0021-9290/$ - see front matter © 2004 Elsevier Ltd. All rights reserved.
doi:10.1016/j.jbiomech.2004.08.024

Considering these limitations, a preferred alternative is to directly measure ground reaction loads using a dynamometric horseshoe.

Design criteria for a dynamometric horseshoe must take specific environmental factors into account. Hoof height varies from 0.9 to 1.0 cm between shoeings (Dyce et al., 1987; Josseck et al., 1995), and a racing plate can be up to 1.8 cm thick with a toe grab (Benoit et al., 1993; Kane et al., 1996) and heel traction devices, leaving a shoe thickness of up to 2.8 cm possible without altering shoeing parameters beyond those found during training. Aluminum racing plates weigh about 0.1 kg (Kane et al., 1996), with their steel training counterparts weighing 0.3 kg. Ideally, the dynamometric horseshoe should be no more than 0.3 kg. The dynamometric horseshoe must be able to withstand at least 1.7 times body weight (BW), or 9000 N with a 550 kg horse, which is representative of the force applied to the legs during high performance activities (Kingsbury et al., 1978; Schamhardt et al., 1993; Kai et al., 1999; Meershoek et al., 2001). A six-load component dynamometer is necessary to completely characterize the ground reaction force and moment vectors for inverse dynamic studies of the equine limb. Finally, to determine the complete load applied to the hoof on a track surface, the dynamometric horseshoe must cover the entire solar surface of the hoof. Moreover, because the contour of the solar surface could affect the pressure distribution and hence the location of the point of application of the ground reaction loads, the contour of the solar surface of the dynamometric horseshoe must be representative of the actual solar surface of Thoroughbred hooves.

Although horse boots (Barrey, 1990) and instrumented horseshoes (Frederick and Henderson, 1970; Roepstorff and Drevemo, 1993; Hjerten and Drevemo, 1994; Roepstorff, 1997; Kai et al., 2000) have been used to determine ground reaction forces, none of these instruments meet the design criteria outlined above particularly the capability to measure all six-load components. Accordingly the first objective of this study was to design and build a dynamometric horseshoe and corresponding instrumentation to satisfy the stated design criteria. The second objective was to perform a static and dynamic calibration to characterize the errors present in the instrument. The final objective was to demonstrate the usefulness of the dynamometric horseshoe by collecting example data from a horse's hoof while walking, trotting, cantering, and galloping.

2. Materials and methods

2.1. Design description

Weighing a total of 0.86 kg, the dynamometric horseshoe that was designed to satisfy the criteria stated above incorporated a pair of parallel plates with three rectangular strain-gaged sensing posts sandwiched between the plates (Fig. 1). The sensing posts, hereafter termed sensors, were positioned with two at the widest part of the dynamometric horseshoe and one at the toe. This placed the COP between the three sensors for most of the stride, specifically where and when the loads were thought to be the greatest (Barrey, 1990; Roepstorff, 1997; Caudron et al., 1998; Wilson et al., 1998). The sensors were designed integral to the hoof plate, which was attached directly to the hoof, and had flanges that were bolted to the ground plate (Fig. 2). The origin of the coordinate system was in the bottom plane of the ground plate and was located in this plane at the centroid of the three sensors. Positive x was in the direction of travel, positive y was in the lateral direction on the left hoof, and positive z was perpendicular to the plates, directed upward when the hoof is on the ground (Fig. 1).

To measure the three force components applied to each sensor, each rectangular post had six strain gage rosettes applied and interconnected to create three full

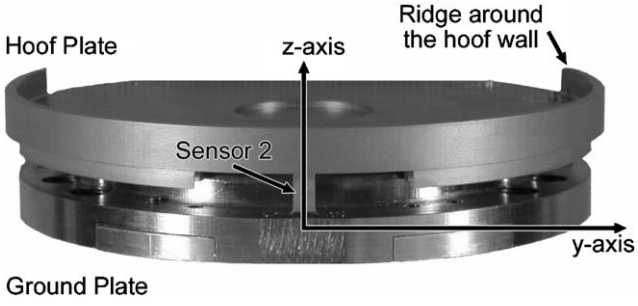

Fig. 1. Dynamometric horseshoe viewed from the toe with coordinate axes superimposed. The x-axis is perpendicular to the plane of the photograph. The elevation of the x–y plane coincides with the bottom plane of the ground plate. The location of the y–z plane is palmar from the center of sensor 2, two-thirds of the distance from sensor 2 to a line between the other two sensors (not visible).

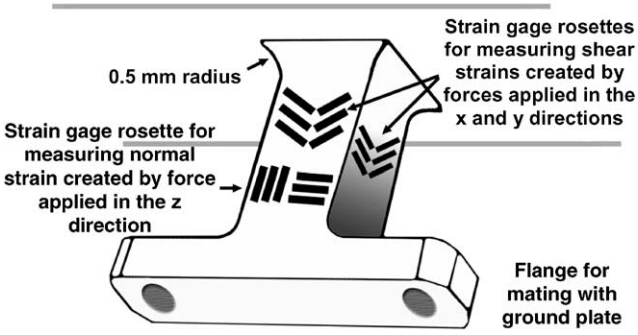

Fig. 2. Diagram indicating strain gage placement on the sensors as viewed from the bottom. Opposite sensor faces have the same gage pattern.

Wheatstone bridge circuits. The z-direction force component was measured by two 350 Ω 90° strain gage rosettes mounted on opposite sides of a post with gages oriented parallel and perpendicular to the axis being measured (Fig. 2). The force components in both the x- and y-directions also were measured with two 350 Ω 90° strain gage rosettes mounted on opposite sides of a post but with the gages oriented at a 45° angle to the z-axis to sense the shear strains developed by the force components. The sensor posts were 0.7 cm high to allow for gage placement. Thus a total of nine Wheatstone bridge voltage outputs designated as Vb_{in} were produced with each output corresponding to one of the three force components applied to each sensor.

The Wheatstone bridge signals were combined to determine the six quantities of interest. The six quantities of interest were the three components of the ground reaction force vector (F_x, F_y, F_z), the ground reaction moment about the z-axis (M_z), and both the x and y coordinates of the COP indicated by X and Y. These six quantities are related to the three components of force developed on each of the sensors through

$$F_x = S_{x1} + S_{x2} + S_{x3}, \tag{1}$$

$$F_y = S_{y1} + S_{y2} + S_{y3}, \tag{2}$$

$$F_z = S_{z1} + S_{z2} + S_{z3}, \tag{3}$$

$$M_z = d_1(S_{x1} - S_{x3}) + (2d_2/3) \times (S_{y2} - S_{y3}/2 - S_{y1}/2), \tag{4}$$

$$M_x = (d_1)(S_{z3} - S_{z1}), \tag{5}$$

$$M_y = (d_2/3)(S_{z1} + S_{z3}) - (2S_{z2}d_2/3), \tag{6}$$

$$X = -M_y/F_z, \tag{7}$$

$$Y = M_x/F_z, \tag{8}$$

where S_{in} are the force components applied to each sensor, i is an index indicating the direction, n is an index indicating the sensor, d_1 is the distance from either sensor 1 or sensor 3 to sensor 2 along the y-axis and d_2 is the distance from either sensor 1 or sensor 3 to sensor 2 along the x-axis. Each Wheatstone bridge signal Vb_{in} represented a corresponding force component S_{in}.

The hoof plate contained both the sensors and the circuitry, and allowed for a range of hoof sizes. The hoof plate was 2.0 mm thick at the thinnest place and was manufactured from titanium. The four points where the dynamometric horseshoe attached to the hoof were slots to allow for a wider variety of hoof sizes and shapes than would be possible with standard holes. The central area internal to the dynamometric horseshoe was indented to allow for flush mounting of a circuit board. When attached to the ground plate, the clearance between the ground plate and the circuit board was 2.0 mm.

The ground plate resembled the shape of the load transfer surface of the hoof as closely as possible. The shape of the ground surface of the ground plate was based on previously reported data describing the solar surface of the hoof (Roland et al., 2003).

The ground plate was stiff in bending to limit the magnitude of force components developed in the x- and y-directions applied to the sensors as a result of any ground plate bending. Using membrane analysis (Roark and Young, 1975), the plate was modeled as a beam of length equal to the distance between the sensors in either the x- or y-direction, 50 or 100 mm, respectively, and width equal to the sensor width, 4.2 mm. Additionally, it was assumed that the ends of the beam were rigidly fixed, that the beam was uniform, and that a point load was applied to the center of the beam. These assumptions led to conservative results. Using this model, horizontal forces in opposing sensors associated with the membrane action of the ground plate (also termed membrane forces) were calculated as 97 and 1527 N in the x- and y-directions, respectively, for a 9000 N point load and a beam thickness of 10 mm (Roland, 2002).

The factor of safety of the sensors was evaluated using the von Mises static failure criterion. The von Mises equivalent stresses for each sensor were calculated for the combined loading condition of both maximal sensor loading (9000 N in z, 1800 N in x and 900 N in y) and maximal horizontal reaction load due to plate bending (97 N in x and 1527 N in y). For a sensor with a square cross section of 0.42 cm, the smallest factor of safety was 2.7.

When the two plates were attached by bolting the sensor flanges to the ground plate, the overall height was 2.1 cm. A sheet metal guard was attached to the ground plate and the internal cavity between the two plates was filled with a low stiffness dielectric gel (SYLGARD™ 527 Silicone, Dow Corning, Midland, MS) that provided a hermetic seal to the electronics but did not interfere with the load transfer. Attachment to the hoof was by means of four screws for secure short-term attachment and easy removal.

Signal conditioning and data acquisition were performed with a custom analog amplification and filter system and a portable computer (Libretto 110, Toshiba, Irvine, CA). Analog signal processing included amplification at a gain of between 100 and 400 (channel dependent) and low pass filtering with a second order active Butterworth filter with a cutoff frequency of 260 Hz. The filtered data were digitized at 1 kHz via a commercial data acquisition card (Model DAQCard AI-16E-4, National Instruments, Austin, TX) and were recorded, analyzed and viewed using customized software (LabVIEW, National Instruments, Austin, TX).

2.2. Calibration and error analysis

Static calibration and error analysis were completed by two methods. In one method, the three force components (F_x, F_y, F_z) and the moment component about the z-axis (M_z) were calibrated using a rigid steel load frame that supported the instrument and allowed attachment of weights via pulleys to apply both forces and couples in positive and negative directions (Davis and Hull, 1981). Higher z forces and forces resulting in moment components about the x- and y-axes (M_x, M_y) were applied using a materials testing system (Model 809, MTS Systems Corporation, Prairie View, MN). Point loads were applied to a 31.8 mm thick steel calibration plate mounted to the dynamometric horseshoe creating a distributed load with a known point of application to induce the required force and moment components.

The load frame was used to apply pure loads. Six force values were applied in the z-direction increasing from 0.3 to 1.1 kN, in 0.16 kN increments, then decreasing to 0.3 kN. Six force values were applied in both the positive and negative x- and y-directions increasing from 0.1 to 0.6 kN in 0.1 kN increments, and decreasing to 0.1 kN. Six positive and six negative values of M_z were applied, increasing from 47 to 198 Nm in 30 Nm increments, and then decreasing to 47 Nm.

The materials testing system was used to apply higher pure z-forces than could be applied with the load frame and z-forces resulting in moment components about the x- and y-axes (M_x, M_y). Pure loads applied in the F_z direction increased in 0.5 kN increments from 1 to 3 kN, then in 1 kN increments up to 9 kN. Moment components about the x- and y-axes were developed by applying F_z loads from 1 to 2.5 kN at locations 2 and 4 cm away from the centroid along the axes to a maximal moment value of 100 Nm. Thus these moment components were applied in combination with a force component in the z-direction. In all cases data was collected for 0.25 s at 1 kHz then averaged.

The sensitivity, linearity, and hysteresis were derived from the static calibration data. The average voltage value was calculated for each raw Wheatstone bridge output for each load condition, then the pre- and post-test zero voltage values were averaged as a baseline and subtracted from the loading test voltage values to get the Wheatstone bridge outputs, Vb_{in}. The Wheatstone bridge voltages were normalized for gain and bridge excitation voltage and mathematically combined to yield the six reduced force and moment voltages using Eqs. (1)–(6). The 36 sensitivities were quantified as the slopes of the regression lines for the reduced voltages versus the applied loads. The quality of the linear model was indicated by the R-squared values. The independent linearity was quantified as the maximum deviation of the reduced voltages from the linear regression line. Output hysteresis was quantified as the maximum reduced voltage deviation from zero voltage output at zero applied load.

Measurement accuracy of the forces and moments, and of the location of the COP, was determined using a well-established procedure for validating multi-load component dynamometers in which a series of known combined loads were applied with very high accuracy (e.g. Hull and Mote, 1978; Hull and Davis, 1981; Macgregor et al., 1985; Newmiller et al., 1988; Hull et al., 1995). A total of 15 different load combinations were applied and the values of the load components were representative of those developed during the various equine gaits. Eight of the load combinations were applied using the load frame, which was specially designed to apply load components with very high accuracy by means of standardized weights (Hull and Davis, 1981), and seven were applied using the materials testing system. These load combinations served as an appropriate gold standard to evaluate the accuracy of our dynamometric horseshoe because the standardized weights were accurate to within $\pm 0.04\%$ and the load cell of the materials testing system was accurate to within $\pm 0.1\%$. The calibration matrix was determined as the inverse of the sensitivity matrix described above and was used to determine the apparent loads and location of the COP. The apparent loads and location of the COP were subtracted from the applied loads and actual location of the COP to determine the error. The total error was quantified by the root mean squared error (RMSE) value presented as a percent of full scale (FS) which corresponded to the greatest magnitude load applied in each direction during the calibration described above.

Finally, a dynamic calibration was performed to determine the natural frequency. The dynamometric horseshoe was attached to a 32-kg mass, which was smaller than that of a horse, but still massive enough to make the mass of the dynamometric horseshoe components insignificant. A piezoelectric accelerometer was attached to the mass, and an impulse was applied to the mass-dynamometric horseshoe system. The period of the vibration was recorded and used to determine the stiffness of the system. The stiffness constant was then used to calculate the expected natural frequency of the dynamometric horseshoe attached to a horse-sized mass of 550 kg.

2.3. Sample equine loading data

To demonstrate the functionality of the dynamometric horseshoe, it was fitted onto the left front hoof of a single subject (Thoroughbred, female, 5 yr old, 490 kg, unfit) while data was collected at the trot (3.0 m/s), canter (6.0 m/s) and gallop (8.0 m/s) on a treadmill (Fig. 3), and at a slow walk (<1.8 m/s) in hand in an

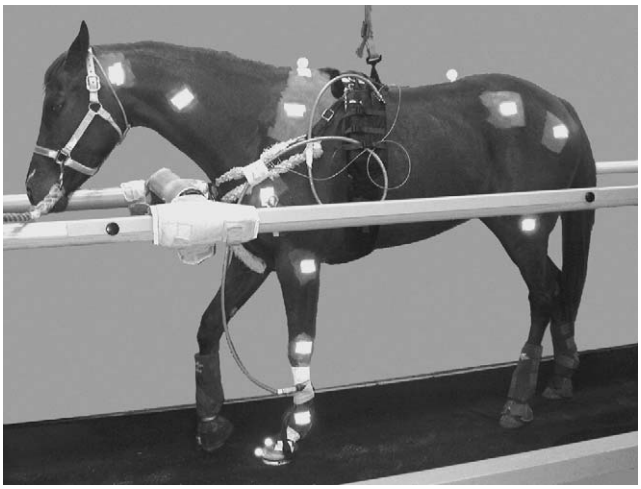

Fig. 3. Photograph of Thoroughbred mare with the dynamometric horseshoe trotting on the treadmill. The reflective markers were not used in the present study.

arena with a hard dirt surface. During the canter and gallop, the dynamometric horseshoe was on the trailing forelimb. The horse wore a pair of weight and height matched forelimb horseshoes for 1 week prior to the testing with the right dummy horseshoe mounted on the contralateral hoof for symmetry during the testing. The hooves were reinforced with an epoxy that was then shaped to mate with the hoof plate of the dynamometric horseshoe. The data acquisition equipment was placed in a pack on the safety surcingle, with the trigger managed by a researcher to the side of the treadmill. Five 10-s trials were collected at the trot and canter, one trial at the gallop, and four trials at the walk. Where available, ten strides were normalized for stride duration and averaged to present a ground reaction force profile. Percents of both stride time in the stance phase and maximal normal force were calculated from the F_z force curves, while percent of stride time spent in positive and negative phases was calculated for the remaining load components. After the equine test, the load frame portion of the accuracy test was repeated to verify that the dynamometric horseshoe was not damaged during use.

3. Results

3.1. Calibration and error analysis

The *R*-squared values for the direct sensitivities exceeded 0.93. The independent linearity ranged from 0.7% to 2.5% FS, with the exception of M_z whose independent linearity was 22.8% FS (Table 1). Output hysteresis was between 0.3% and 2.0% for the force components but increased to 18% for M_z. Because F_z had the lowest independent linearity and hysteresis, F_z also had the lowest RMSE of 3.5% FS. Because M_z had the largest independent linearity and hysteresis, the RMSE for M_z was also the largest at 13.6% FS.

The dynamic test in conjunction with the subsequent computations demonstrated that the natural frequency of the horseshoe was 1744 Hz for a 550 kg horse.

3.2. Sample equine loading data

The ground reaction loads depended on the gait of the horse. The F_z force profile at the walk demonstrated the traditional double peak in the stance phase, which encompassed 70% of the 1.22 s mean stride time (SD $\pm$ 0.10 s) (Fig. 4). The peak average F_z force was 2617 N. Stance phase at the trot was 46% of the 0.68 s mean stride time (SD $\pm$ 0.02 s) and the peak average F_z was 3040 N, which exceeded that of the walk by 16%. Stance phase at the canter was 36% of the 0.50 s mean stride time (SD $\pm$ 0.01 s) and the peak average F_z force was 4626 N, which exceeded that of the walk by 77%. At the gallop, the stance phase was 60% of the 0.85 s mean stride time (SD $\pm$ 0.4 s) and the peak average F_z force was 2917 N, which was 11% greater than the peak average F_z force at the walk.

Differences were also evident in the other load components depending on the gait of the horse. The patterns at the walk, trot, and canter were similar in that F_x was negative for about the first half of the stance phase and positive for the majority of the remainder of the stance phase and the negative and positive extreme values differed by less than a factor of 2 within a gait type (Fig. 4). In contrast to these three gaits, the F_x force profile for the gallop was characterized by a much lower magnitude negative phase with a minimum of only -86 N and a high magnitude positive phase with a maximum of 435 N, which was 5 times greater in magnitude than the negative extreme.

F_y was always the smallest of the three force components (Fig. 4) being less than 80 N at the walk and predominantly negative with a minimum of –128 N at the trot. At the canter F_y showed a large negative peak of -475 N in the first 2% of stance phase, and then oscillated with low magnitude about zero. F_y was negative with a flat minimum of -90 N, showing little change throughout the stride at the gallop.

The extreme values of the torsional moment M_z were large in magnitude for all four gaits (Fig. 4). At the walk, trot, canter, and gallop the maximum magnitudes were 40 Nm (positive extreme), 63 Nm (positive extreme), 76 Nm (negative extreme), and 65 Nm (positive extreme), respectively.

The COP at the walk occurred initially near the centroid of the sensors, deviated about 2 cm laterally and palmarly, where it remained for almost 85% of the stance phase, and then moved dorsally along the *x*-axis

Table 1
Measures of dynamometric horseshoe performance computed from the calibration and accuracy check

Performance measure	F_z	F_x	F_y	M_z	M_x	M_y	X	Y
Independent linearity	0.7%	2.0%	1.6%	22.8%	1.7%	2.5%	NA	NA
Hysteresis	0.3%	0.9%	2.0%	18.0%	NA	NA	NA	NA
Absolute RMSE	325 N	54 N	56 N	27 Nm	5 Nm	4 Nm	0.5 mm	0.6 mm
Relative RMSE	3.5%	9.0%	9.4%	13.6%	5.1%	3.8%	12.3%	15.6%

All percents are relative to the maximum value applied during the calibration. Maximum values were 9000 N for F_z, 600 N for F_x and F_y, 198 Nm for M_z, 100 Nm for M_x and M_y, and 4 cm for both X and Y.

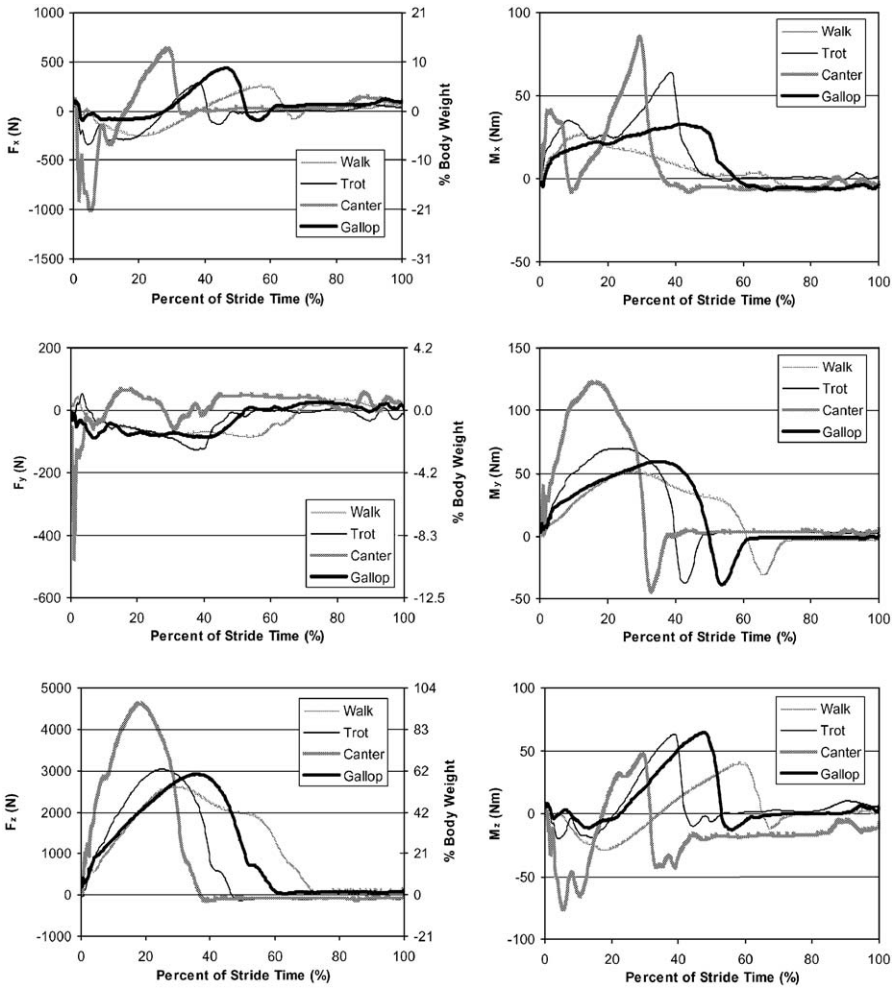

Fig. 4. Comparison of average ground reaction force and moment profiles for the four gaits of a 490 kg Thoroughbred mare. The walking, trotting, cantering, and galloping speeds were 1.8, 3.0, 6.0, and 8.0 m/s, respectively.

at toe off (Fig. 5). In contrast, the COP at the trot initiated laterally and palmarly, moved towards the centroid nearing the x-axis about 2 cm behind the origin, then moved along an arc on the lateral perimeter of the horseshoe with the COP at toe off occurring about 4 cm lateral of the x-axis. The error in the trace is evident in the last 25% of the stance phase where the trace traveled laterally off, and then dorsal to, the dynamometric horseshoe. The COP at the canter also initiated laterally and palmarly, remained in that quadrant for 82% of the stance phase, then again moved along an arc laterally 4 cm and returned 2 cm lateral to the x-axis dorsal to the horseshoe at toe off. In contrast, the COP at the gallop occurred medially and palmarly at the initiation of the stance phase, moved laterally to about 2 cm lateral of the origin where it was located for 67% of the stance phase, before traveling dorsally to the toe of the horseshoe, crossing to about 1 cm medial again at toe off.

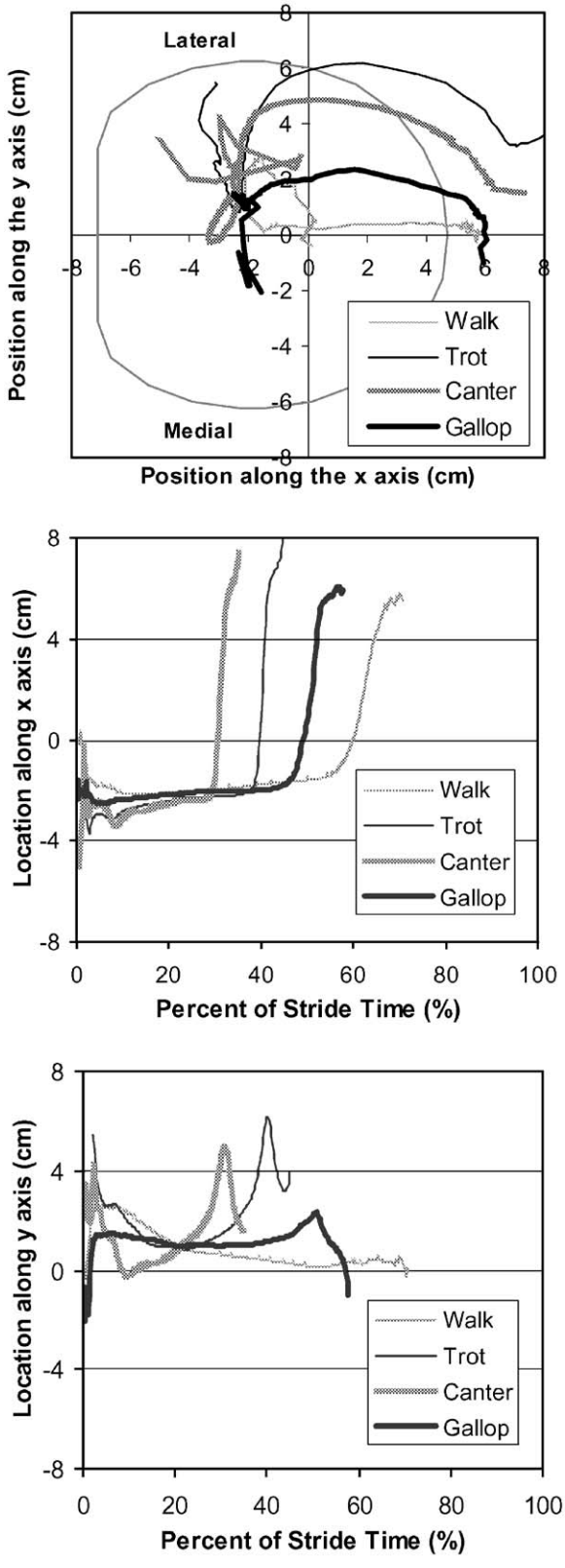

Fig. 5. Comparison of X and Y coordinates of the COP and location of the COP on the solar surface of the hoof for the four gaits of a 490 kg Thoroughbred mare. The walking, trotting, cantering, and galloping speeds were 1.8, 3.0, 6.0, and 8.0 m/s, respectively.

4. Discussion

Although knowledge of ground reaction loads is the basis for biomechanical analysis and prevention of musculoskeletal injuries in racehorses, no previous study known to the authors has developed a dynamometric horseshoe that could be used to measure the complete ground reaction force and moment vector during racing conditions. Therefore the objectives of this study were (1) to design and fabricate, (2) to evaluate the performance of, and (3) to demonstrate the usefulness of a dynamometric horseshoe capable of measuring the complete ground reaction force and moment vector during training on a track surface. The key findings were (1) a six-load component dynamometric horseshoe was designed whose weight and height were 0.86 kg and 2.1 cm, respectively, (2) the RMSE was less than 5% FS for F_z, M_x, and M_y but increased to 9–13% for F_x, F_y, and M_z, (3) the natural frequency was 1744 Hz, and (4) the six-load components were measured during walking, trotting, cantering, and galloping. Because the success of this project can be gauged by assessing how well the instrument satisfied the design requirements, the design will be critically evaluated against each of the requirements followed by a discussion of the sample data.

4.1. Design requirements

The 2.1-cm height of the dynamometric horseshoe was within the 2.8 cm design requirement, but the 0.86 kg weight exceeded the 0.3 kg mass of a training horseshoe. Accordingly, consideration of the possible effects that this excess weight could have on the system being measured is warranted. Additional mass at the hoof level affects the segment kinematics of the swing phase as a result of the linear accelerations (Lanovaz et al., 1999). Also a comparison of the moment of inertia of the forelimb calculated about the elbow indicated that moment of inertia of the forelimb plus the dynamometric horseshoe was 1.68 kg-m^2, which represented an increase in the moment of inertia of 0.35 kg-m^2 above the moment of inertia of the forelimb plus training plate. An increase in moment of inertia of 0.06 kg-m^2 in Standardbred trotters did not change temporal stride characteristics, but did create horse specific alterations in forelimb joint kinematics (Willemen et al., 1994). Collectively, these two studies support the idea that the mass of the dynamometric horseshoe could affect stride variables being studied.

The specified loading limits were derived using data from the literature. The total force in the z-direction has been measured on horses during canter (Kai et al., 1999, 2000) and during faster gallop (Kingsbury et al., 1978) with a maximum force of 1.7 BW. In addition, data has been collected from sport horses landing off of a 1-m jump (Schamhardt et al., 1993; Meershoek et al., 2001)

with the maximal ground reaction force in the trailing forelimb being about 1.5 BW in most cases. For an equine mass of 550 kg, the maximal design force in the z-direction was 9000 N.

Studies that have examined the other force components indicate that the maximal force in the fore-aft direction is 20% of the maximal force in the z-direction (Roepstorff and Drevemo, 1993; Schamhardt et al., 1993; Hjerten and Drevemo, 1994; Johnston, 1997; Roepstorff, 1997). Accordingly, the maximal design force in the fore-aft direction was 1800 N in our case. The one study that mentions gathering the medial-lateral component of the ground reaction force commented that the changes were too small to be relevant (Roepstorff, 1997), so for our estimation we used 10% of the maximal force in the z-direction as the design force in the y-direction. The dynamometric horseshoe was loaded to these levels for the various force components and had a linear output for all six quantities measured.

At 3.5% FS, the RMSE in the F_z direction was the smallest error of the force components. The errors present in the F_x and F_y load components were larger. Because M_z was computed from the outputs used to compute both F_x and F_y, the error was largest in the M_z load component. However, the importance of M_z in the etiology of musculoskeletal injuries has not been established. M_x and M_y quantities had smaller errors than M_z because they were computed from the outputs used to compute F_z.

The error of the location of the COP ranged from 12% to 16% FS in both coordinates for loads applied within 4 cm of the origin and F_z greater than 400 N. The errors for the location of COP for no applied load in the z-direction were omitted because as F_z approaches zero in the denominator in Eqs. (7) and (8), any cross talk resulting in a non-zero value in either M_x or M_y will cause the values of X and Y to approach infinity (Barrey, 1990; Bobbert and Schamhardt, 1990). Minimal load for determining the location of the COP is generally taken to be 1000 N (Bobbert and Schamhardt, 1990), but all data that appeared reasonable was presented in this paper, with the minimal F_z values used to determine the location of the COP above 200 N in most cases.

Measurement errors of this dynamometric horseshoe were similar to those of other dynamometric horseshoes, and also other devices used to determine ground reaction loads. Some dynamometric horseshoes had incomplete descriptions of accuracy tests and results (Frederick and Henderson, 1970; Barrey, 1990; Ratzlaff et al., 1990; Roepstorff, 1997). Relative errors for Kistler force platforms (type 9287) ranged from 1.6% FS in F_z to a cross talk of 3.5% FS of F_z in F_x and F_y (Bobbert and Schamhardt, 1990). Other custom instruments had RMSEs ranging from 3.7% FS to 6.8% FS and relative errors of 5–9.3% for the F_z load component with an applied load only in F_z and RMSEs of 3.3% FS to 3.4% FS for the F_x load component with an applied load only in F_x (Bjorck, 1957–58; Kai et al., 2000). Comparison of instrument performance was difficult because accuracy testing and reporting are not standardized.

Because the ground reaction loading is dynamic, with loading and unloading taking place in less than 0.1 s, the natural frequency of the dynamometric horseshoe was determined to ensure that apparent loads computed using the static calibration were relatively unaffected by the dynamic response. The natural frequency of 1744 Hz was more than five times greater than the 260 Hz cutoff frequency, a bandwidth considered sufficient for the study of the hoof strike at a gallop (Benoit et al., 1993). Because the usable bandwidth of an undamped second order system is about 20% of the natural frequency without the need to correct for instrument dynamics (Doebelin, 1990), the natural frequency was sufficiently high.

Simple attachment and removal of the dynamometric horseshoe were required to prevent damage to the instrument and were achieved by attaching the dynamometric horseshoe to the hoof with screws. One limitation with the hoof plate design is that because there is only a limited amount of room for size variation, horses intended as possible subjects must be screened to insure that the horseshoe can accommodate their hoof size.

Because force can be transferred between the hoof and the ground at all areas of contact particularly on racing surfaces, the ground plate of the dynamometric horseshoe had to cover the entire area of the ground surface of the hoof to be used on track surfaces. To meet this requirement, the ground plate covered the entire area of the hoof and mimicked the contours of the solar surface of the hoof as well.

4.2. Example data

Comparisons of the example load component profiles presented herein to those previously reported particularly from force plates should be made with caution for several reasons. One reason is that the load components measured by the dynamometric horseshoe are not the same as those measured by a force plate. This is because the dynamometric horseshoe measures load components in a local coordinate system fixed to the hoof whereas a force plate measures load components in a laboratory coordinate system fixed to the ground. Because these two coordinate systems are not in general aligned, a direct comparison between load components cannot be made. A second reason is that the conditions of our tests may have been different from those previously reported. Because both the type of surface and speed would affect the load components, any differences in these conditions

between tests further complicates direct comparisons (Kai et al., 1999). A final reason is that the example load component profiles presented herein are for a single subject. As such, these load component profiles may be unique to this subject and may not be typical of the population.

In view of these reasons, any comparisons should be restricted to the patterns of the various load components rather than the magnitudes. Furthermore differences between our patterns and those provided by force plates may be evident because of the differences in the coordinate systems. Finally comparisons of the force profiles in galloping cannot be made owing to a lack of results for this type of gait in the literature other than the single study with which the authors are aware that provided only the force profile for F_z (Kingsbury et al., 1978).

In considering first the walk, the patterns of the force and moment component profiles were generally similar to those in the literature with a few exceptions. The F_z force profile at the walk showed the characteristic double peak, with the first peak being greater than the second peak (Fig. 4). Similarly, force profiles collected using force plates also demonstrate the characteristic double peak but with either both peaks equal or the second peak higher (Merkens et al., 1985; Schamhardt and Merkens, 1987; Hodson et al., 2000). This difference could be due to either our subject or the different surfaces used; in our study the subject walked on a dirt surface whereas in the previous studies the horse walked on a hard surface.

The F_x force profile at the walk exhibited predominantly a two-phase pattern with a negative phase lasting approximately half of the stance phase followed by a positive phase lasting for most of the remaining half of the stance phase. This pattern is similar to those previously reported using force plates (Merkens et al., 1985; Schamhardt and Merkens, 1987; Hodson et al., 2000) with one difference. Namely the F_x force profile for the dynamometric horseshoe showed a negative force applied during the last 7–12% of the stance phase. This difference is likely traced to the local coordinate system attached to the hoof in which our dynamometric horseshoe measured loads. As soon as the hoof began to lift off the ground, the application of force normal to the ground became apparent as a negative force in the F_x direction. This pattern is typical of instruments attached to the hoof.

The pattern of F_y at the walk was negative for most of the stance phase with a small positive excursion just before toe off. Again this is similar to patterns of F_y previously reported using force plates (Merkens et al., 1985; Schamhardt and Merkens, 1987; Hodson et al., 2000) with the small positive excursion sometimes being either present or absent depending on the subject. Also in agreement with previous studies, the F_y force component was the smallest in magnitude of the three force components.

The patterns of all three force components at the trot and canter were generally similar to those previously reported using force plates (Merkens et al., 1993a,b; Clayton et al., 1999; Kai et al., 1999; Roepstorff et al., 1999). The F_z force profiles were well characterized by a half-sinusoid shape whose magnitude was greater for the canter than the trot, the F_x force profiles for both the canter and the trot were predominantly biphasic, and the F_y force profile for the trot was unipolar for the most part and substantially smaller in magnitude than the other two force components. As with the walk, the F_x force profiles at the trot exhibited a negative region applied during the last 10–15% of the stance phase presumably for the same reason (i.e. local coordinate system).

5. Conclusions

The primary advancements of our dynamometric horseshoe over those described previously are (1) the ability to measure the complete ground reaction loads, (2) the ability to replicate the actual loads applied to a hoof by matching the solar surface of the dynamometric horseshoe to that of a horse's hoof, and (3) quantified measurement accuracy for all six-load components. While offering these advancements, the dynamometric horseshoe satisfied most of the stated design criteria and provided both accuracy and force profiles comparable to those of other instruments used for measuring the ground reaction loads in horses. Moreover, the use of the dynamometric horseshoe under racing conditions was demonstrated. Accordingly, the dynamometric horseshoe is a new instrument that can be used to measure loads that are difficult to measure with conventional instruments such as force plates. As such the dynamometric horseshoe should prove useful for the study of factors, which affect ground reaction loads for the Thoroughbred population during racing conditions.

Acknowledgements

We are grateful to the Grayson Jockey Club Research Foundation for providing the financial support for this study.

References

Balch, O.K., Helman, R.G., Collier, M.A., 2001. Underrun heels and toe-grab length as possible risk factors for catastrophic musculoskeletal injuries in Oklahoma racehorses. Proceedings of the 47th Annual Meeting of the American Association of Equine Practitioners, vol. 47, pp. 334–338.

Barr, A.R., Dow, S.M., Goodship, A.E., 1995. Parameters of forelimb ground reaction force in 48 normal ponies. Veterinary Record 136, 283–286.

Barrey, E., 1990. Investigation of the vertical hoof force distribution in the equine forelimb with an instrumented horseboot. Equine Veterinary Journal Supplement 9, 35–38.

Benoit, P., Barrey, E., Regnault, J.C., Brochet, J.L., 1993. Comparison of the damping effect of different shoeing by the measurement of hoof acceleration. Acta Anatomica 146, 109–113.

Bjorck, G., 1957–58. Studies on the draught force of horses: development of a method using strain gauges for measuring forces between hoof and ground. Acta Agriculturae Scandinavica 8, 110.

Bobbert, M.F., Schamhardt, H.C., 1990. Accuracy of determining the point of force application with piezoelectric force plates. Journal of Biomechanics 23, 705–710.

Caudron, I., Grulke, S., Farnir, F., Vanschepdael, P., Serteyn, D., 1998. In-shoe foot force sensor to assess hoof balance determined by radiographic method in ponies trotting on a treadmill. Veterinary Quarterly 20, 131–135.

Clayton, H., Lanovaz, J.L., Schamhardt, H.C., Van Wessum, R., 1999. The effects of a rider's mass on ground reaction forces and fetlock kinematics at the trot. Equine Veterinary Journal Supplement 30, 218–221.

Davis, R.R., Hull, M.L., 1981. Measurement of pedal loading in bicycling, I. Instrumentation. Journal of Biomechanics 14, 843–856.

Doebelin, E.O., 1990. Measurement Systems: Application and Design, fourth ed. McGraw-Hill, New York, NY.

Dyce, K.M., Sack, W.A., Wensing, C.J.G., 1987. Textbook of Veterinary Anatomy. W.B. Saunders Co., Philadelphia, PA.

Estberg, L., Stover, S.M., Gardner, I.A., Johnson, B.J., Jack, R.A., Case, J.T., Ardans, A., Read, D.H., Anderson, M.L., Barr, B.C., Daft, B.M., Kinde, H., Moore, J., Stoltz, J., Woods, L., 1998. Relationship between race start characteristics and risk of catastrophic injury in Thoroughbreds: 78 cases (1992). Journal of the American Veterinary Medical Association 212, 544–549.

Frederick Jr., F.H., Henderson, J.M., 1970. Impact force measurement using preloaded transducers. American Journal of Veterinary Research 31, 2279–2283.

Hill, A.E., Carpenter, T.E., Gardner, I.A., Stover, S.M., 2003. Evaluation of a stochastic Markov-chain model for the development of forelimb injuries in Thoroughbred racehorses. American Journal of Veterinary Research 64, 328–337.

Hill, A.E., Stover, S.M., Gardner, I.A., Kane, A.J., Whitcomb, M.B., Emerson, A.G., 2001. Risk factors for and outcomes of noncatastrophic suspensory apparatus injury in Thoroughbred racehorses. Journal of the American Veterinary Medical Association 218, 1136–1144.

Hjerten, G., Drevemo, S., 1994. Semi-quantitative analysis of hoof-strike in the horse. Journal of Biomechanics 27, 997–1004.

Hodson, E., Clayton, H.M., Lanovaz, J.L., 2000. The forelimb in walking horses: 1. Kinematics and ground reaction forces. Equine Veterinary Journal 43, 287–294.

Hull, M.L., Brewer, R., Hawkins, D., 1995. A new force plate design incorporating octagonal strain rings. Journal of Applied Biomechanics 11, 311–321.

Hull, M.L., Davis, R.R., 1981. Measurement of pedal loading in bicycling. 1. Instrumentation. Journal of Biomechanics 14, 843–856.

Hull, M.L., Mote, C.D., 1978. Analysis of leg loading in snow skiing. Journal of Dynamic Systems Measurement and Control 100, 177–186.

Johnson, B.J., Stover, S.M., Daft, B.M., Kinde, H., Read, D.H., Barr, B.C., Anderson, M., Moore, J., Woods, L., Stoltz, J., et al., 1994. Causes of death in racehorses over a 2 year period. Equine Veterinary Journal 26, 327–330.

Johnston, C., 1997. On the kinematics and kinetics of the distal limb in the Standardbred trotter. Ph.D. Dissertation, Department of Anatomy and Histology, University of Agricultural Sciences, Uppsala, Sweden.

Josseck, H., Zenker, W., Geyer, H., 1995. Hoof horn abnormalities in Lipizzaner horses and the effect of dietary biotin on macroscopic aspects of hoof horn quality. Equine Veterinary Journal 27, 175–182.

Kai, M., Aoki, O., Hiraga, A., Oki, H., Tokuriki, M., 2000. Use of an instrument sandwiched between the hoof and shoe to measure vertical ground reaction forces and three-dimensional acceleration at the walk, trot, and canter in horses. American Journal of Veterinary Research 61, 979–985.

Kai, M., Takahashi, T., Aoki, O., Oki, H., 1999. Influence of rough track surfaces on components of vertical forces in cantering Thoroughbred horses. Equine Veterinary Journal Supplement 30, 214–217.

Kane, A.J., Stover, S.M., Gardner, I.A., Case, J.T., Johnson, B.J., Read, D.H., Ardans, A.A., 1996. Horseshoe characteristics as possible risk factors for fatal musculoskeletal injury of Thoroughbred racehorses. American Journal of Veterinary Research 57, 1147–1152.

Kane, A.J., Stover, S.M., Gardner, I.A., Bock, K.B., Case, J.T., Johnson, B.J., Anderson, M.L., Barr, B.C., Daft, B.M., Kinde, H., Larochelle, D., Moore, J., Mysore, J., Stoltz, J., Woods, L., Read, D.H., Ardans, A.A., 1998. Hoof size, shape, and balance as possible risk factors for catastrophic musculoskeletal injury of Thoroughbred racehorses. American Journal of Veterinary Research 59, 1545–1552.

Kingsbury, H.B., Quddus, M.A., Rooney, J.R., Geary, J.E., 1978. A laboratory system for production of flexion rates and forces in the forelimb of the horse. American Journal of Veterinary Research 39, 365–369.

Lanovaz, J.L., Clayton, H., Colborne, G.R., Schamhardt, H.C., 1999. Forelimb kinematics and net joint moments during the swing phase of the trot. Equine Exercise Physiology Supplement 30, 235–239.

Lindner, A., Dingerkus, A., 1993. Incidence of training failure among Thoroughbred horses at Cologne, Germany. Preventive Veterinary Medicine 16, 85–94.

Macgregor, D., Hull, M.L., Dorius, L.K., 1985. A microcomputer controlled snow ski binding system. 1. Instrumentation and field-evaluation. Journal of Biomechanics 18, 255–265.

Meershoek, L.S., Roepstorff, L., Schamhardt, H.C., Johnston, C., Bobbert, M.F., 2001. Joint moments in the distal forelimbs of jumping horses during landing. Equine Veterinary Journal 33, 410–415.

Merkens, H.W., Schamhardt, H.C., Hartman, W.R., Kersjes, A.W., 1985. Ground reaction force patterns of Dutch Warmblood horses at normal walk. Equine Veterinary Journal 18, 207–214.

Merkens, H.W., Schamhardt, H.C., van Osch, G.J., Hartman, W., 1993a. Ground reaction force patterns of Dutch Warmbloods at the canter. American Journal of Veterinary Research 54, 670–674.

Merkens, H.W., Schamhardt, H.C., Van Osch, G.J., Van den Bogert, A.J., 1993b. Ground reaction force patterns of Dutch Warmblood horses at normal trot. Equine Veterinary Journal 25, 134–137.

Newmiller, J., Hull, M.L., Zajac, F.E., 1988. A mechanically decoupled 2 force component bicycle pedal dynamometer. Journal of Biomechanics 21, 375–386.

Pratt Jr., G.W., O'Connor Jr., T., 1976. Force plate studies of equine biomechanics. American Journal of Veterinary Research 37, 1251–1255.

Ratzlaff, M.H., Hyde, M.L., Grant, B.D., Balch, O., Wilson, P.D., 1990. Measurement of vertical forces and temporal components of the strides of horses using instrumented shoes. Equine Veterinary Science 10, 23–35.

Roark, R.J., Young, W.C., 1975. Formulas for Stress and Strain, fifth ed. McGraw-Hill, New York, NY.

Roepstorff, L., 1997. A force measuring horseshoe applied in kinetic and kinematic analysis of the trotting horse. Ph.D. Dissertation, Department of Large Animal Clinical Sciences, Swedish University of Agricultural Sciences, Uppsala, Sweden.

Roepstorff, L., Drevemo, S., 1993. Concept of a force-measuring horseshoe. Acta Anatomica 146, 114–119.

Roepstorff, L., Johnston, C., Drevemo, S., 1999. The effect of shoeing on kinetics and kinematics during the stance phase. Equine Veterinary Journal Supplement 30, 279–285.

Roland, E.S., 2002. A dynamometric horseshoe for measuring the complete ground reaction load at racing speeds on racing surfaces. M.S. Thesis, Biomedical Engineering Program, University of California at Davis.

Roland, E.S., Stover, S.M., Hull, M.L., Dorsch, K., 2003. Geometric symmetry of the solar surface of hooves of Thoroughbred racehorses. American Journal of Veterinary Research 64, 1030–1039.

Rossdale, P.D., Hopes, R., Wingfield Digby, N.J., Offord, K., 1985. Epidemiological study of wastage among racehorses 1982 and 1983. Veterinary Record 116, 66–69.

Schamhardt, H.C., Merkens, H.W., 1987. Quantification of equine ground reaction force patterns. Journal of Biomechanics 20, 443–446.

Schamhardt, H.C., Merkens, H.W., Vogel, V., Willekens, C., 1993. External loads on the limbs of jumping horses at take-off and landing. American Journal of Veterinary Research 54, 675–680.

Steiss, J.E., Yuill, G.T., White, N.A., Bowen, J.M., 1982. Modifications of a force plate system for equine gait analysis. American Journal of Veterinary Research 43, 538–540.

Willemen, M.A., Savelberg, H.H.C.M., Bruin, G., Barneveld, A., 1994. The effect of toe weights on linear and temporal stride characteristics of Standardbred trotters. Veterinary Quarterly 16 (Supplement 2), S97–S100.

Wilson, A.M., Seelig, T.J., Shield, R.A., Silverman, B.W., 1998. The effect of foot imbalance on point of force application in the horse. Equine Veterinary Journal 30, 540–545.